Fano resonance in a cholesteric liquid crystal with dye

A. H. Gevorgyan*
Department of Physics, Yerevan State University, 1 Alex Manoogian Street, 0025 Yerevan, Armenia

(Received 31 August 2018; published 25 January 2019)

In this paper, we consider the optical properties of cholesteric liquid crystals (CLCs) with a dye. We investigate the reflection, transmission, and absorption spectra peculiarities. We show that in the presence of dye molecules, in certain conditions, the photonic band gap (PBG) splits into two, three, etc., PBGs. A simple geometric method for determination of the Bragg frequencies and the widths of forbidden bands is proposed. It is shown that we can change the Bragg frequencies and the widths of forbidden bands by changing the parameters of dye molecules. We investigate the light localization peculiarities in the CLC layer in the presence of dye molecules. The peculiarities of the spectra of the photonic density of states and the spectra of light energy density in the CLC layer are also investigated. We show that in the presence of two types of resonances the observation of Fano resonance is possible. The peculiarities of Fano resonance in the CLC with dyes are investigated. We show that this system can be used for achieving a narrow bandwidth spectral response in transmission or reflection.

DOI: 10.1103/PhysRevE.99.012702

I. INTRODUCTION

Fano resonance is a type of resonant scattering phenomenon that gives rise to an asymmetric line shape and is a universal phenomenon throughout physics [1]. As it is well known, for many years, the Lorentzian formula was regarded as the fundamental line shape of a resonance. Moreover, for many phenomena taking place in the presence of several independent resonances of different physical origin, the line shape is simply the sum of the intensities of the individual resonances that contribute to it. In other words, interference effects due to interacting resonances are absent in the most typical resonance phenomena. The microscopic origin of the Fano resonance arises from the constructive and destructive interference of a narrow discrete resonance with a broad spectral line or a continuum [2]. After its discovery, a large number of studies were conducted on the Fano resonances in various quantum systems, such as quantum dots, nanowires, and tunneling compounds (see the review article [3]). The Fano resonance has generally been regarded as a feature entirely specific to quantum systems. However, the phenomena of such interference of the wave function have analogies in classical optics. The first observation of this asymmetric line shape in optics is probably Wood's anomaly [4]; however, a clear understanding that this phenomenon is related to the interference of excited leaky modes with incoming radiation took some time to emerge. Recently it has been shown that the asymmetric profiles of this effect agree well with the Fano formula [5]. Nowadays, Fano resonances have been widely investigated in nanoscale structures [2,6], including in nanoplasmonic structures [2,7–10], and dielectric or semiconductor systems [11], such as photonic crystals (PCs) [12–14], slabs [15,16], photoemitters [17], indirect coupling cavities [18], and coupled cavity systems [19–21]. The dispersion of the Fano resonance profile finds applications in sensors, lasing, switching, and nonlinear and slow-light devices, and finally in many photonic and spectroscopic devices.

In this paper, we investigate the peculiarities of the resonant scattering of light in cholesteric liquid crystals (CLCs) in the presence of dye molecules.

CLCs have a self-organized helical structure which can be regarded as a one-dimensional PC. The periodic structure of CLCs gives rise to a polarization-sensitive photonic band gap (PBG). The PBG of the CLCs is defined by the condition $n_o p < \lambda < n_e p$, where p is its helix pitch, and n_o and n_e are the ordinary and extraordinary local refractive indices. Within the PBG only the circularly polarized light having the same handedness as the CLC helix is selectively reflected (of course at normal light incidence). The light polarized with the opposite handedness does not diffract on its periodical structure. The CLC parameters can easily be tuned by external electric, magnetic, or light fields, or by a thermal gradient, or an infrared radiation, etc. A suitable manipulation of the CLC layer parameters allows fine tuning of their PBG and other characteristics.

Liquid crystalline suspensions of various micro- or nanoparticles or dye molecules have recently been the subject of renewed interest because they combine the fluidity and anisotropy of liquid crystals with the specific properties of the particles or dye molecules. The presence of nanoparticles (either ferroelectric, or ferromagnetic) or dye molecules in a CLC structure leads to an essential increase or decrease of its local (both dielectric and magnetic) anisotropy; a significant change of the *isotropic phase–liquid phase* transition temperature; a significant change of the photonic band-gap frequency width and the frequency localization; a change of numbers of PBGs; a change of the CLC elasticity coefficients; a significant increase of the CLC tuning possibilities, etc. [22,23]. In the review article [24] the peculiarities of the diffraction of an electromagnetic wave on a periodic condensed matter where the Bragg condition is satisfied at the frequency of

*agevorgyan@ysu.am

resonance excited in this medium were considered. In addition, in [25], the spectral properties of a one-dimensional PC with a defect nanocomposite layer that consists of metallic nanoballs distributed in a transparent matrix and is characterized by an effective resonance permittivity are studied.

II. MODEL AND METHODOLOGY

Let us consider light propagation in a CLC along its helix axis. The dielectric permittivity, $\hat{\varepsilon}$, and magnetic permeability, $\hat{\mu}$, tensors have the form

$$\hat{\varepsilon}(z) = \varepsilon_m \begin{pmatrix} 1+\delta\cos(2az) & \pm\delta\sin(2az) & 0 \\ \pm\delta\sin(2az) & 1-\delta\cos(2az) & 0 \\ 0 & 0 & 1-\delta \end{pmatrix},$$
$$\hat{\mu}(z) = \hat{I}, \tag{1}$$

where $a = 2\pi/p$, p is the helix pitch, $\varepsilon_m = (\frac{\varepsilon_1+\varepsilon_2}{2})$, $\delta = (\frac{\varepsilon_1-\varepsilon_2}{\varepsilon_1+\varepsilon_2})$, ε_1 and ε_2 are diagonal elements of the local dielectric tensor, and $\hat{I}$ is the unit matrix. We characterize the degree of an arrangement of dipole transition momenta of the guest molecules by the order parameter, S_d, defining it through the average of $\cos\vartheta$: $S_d = \frac{3}{2}\langle\cos\vartheta\rangle - \frac{1}{2}$, where ϑ is the angle between the local optical axis of the CLC and the dipole transition momentum of the guest dye molecule. The possible maximum value of this order parameter is the unit $S_d = 1$ and it corresponds to the ideal orientation of the transition dipole momenta along the local optical axis; the isotropic (chaotic) orientation of transition dipole momenta corresponds to the value $S_d = 0$, and the minimum value $S_d = -0.5$ corresponds to the distribution of those momenta in the plane, which are perpendicular to the local optical axis. Here we assume $S_d = 0$. In this case, in the presence of dye molecules in the CLC matrix, the main values of the local dielectric tensor will stand frequency dependent, and we here assume the Lorentzian form of their frequency dependence, i.e., we assume that

$$\varepsilon_{1,2}(\omega) = \varepsilon^0_{1,2} + \frac{f_{1,2}}{\omega^2_{01,2} - \omega^2 - i\gamma_{1,2}\omega}, \tag{2}$$

where $\gamma_{1,2}$ are the broadenings of resonance absorption lines or simply damping factors, $f_{1,2}$ are the quantities proportional to oscillator strengths, $\omega_{01,2}$ are the resonance frequencies, $\varepsilon^0_{1,2}$ are parts of dielectric permittivities not depending on frequency, and i is the imaginary unit.

We will consider the light transmission and reflection at its normal incidence (the incidence angle is zero) on a planar layer of the CLC. The analytical solution of this boundary problem is given in [26], and we will use some results from this paper for numerical simulations.

We will consider a normal light incidence on the half space of the CLC, too. The analytical solution of this boundary problem is given in [27], and we will use some results from this paper as well for numerical simulations.

III. RESULTS

Let us consider light reflection and transmission through a CLC layer of finite thickness. In Fig. 1 the reflection spectra of the light reflected from the CLC layer of finite thickness

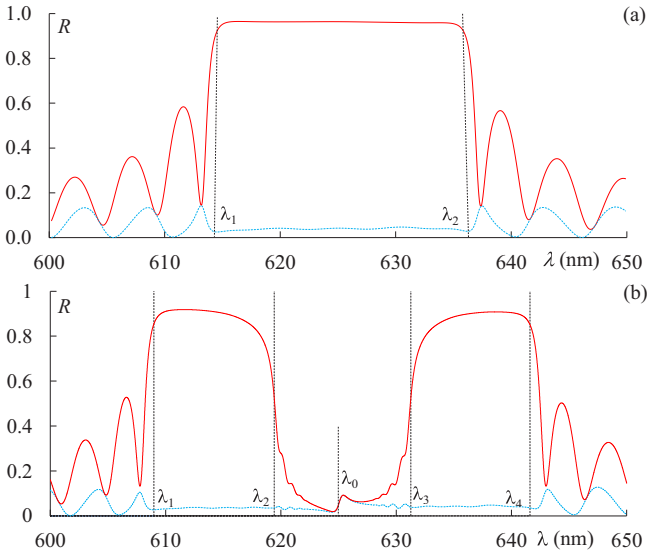

FIG. 1. The reflection spectra in the absence of dye molecules in the CLC matrix (a) and in their presence (b). $\omega_{01} = \omega_{02} = \omega_B = \frac{ac}{\sqrt{\varepsilon_m}}$, where c is light speed in a vacuum. The incident light is RCP (the red solid lines) and LCP (the blue dashed lines). The other parameters are $p = 420\,\text{nm}$, $\varepsilon^0_1 = 2.29$, $\varepsilon^0_2 = 2.143$, $B = f_1 = f_2 = 2\times10^{28}\text{s}^{-2}$, $\gamma = \gamma_1 = \gamma_2 = 4\times10^{12}\text{s}^{-1}$, and CLC layer thickness $d = 50p$.

bordered with a vacuum on both its sides (that is, when $\varepsilon_s = 1$, where ε_s is the dielectric permittivity of the CLC layer surroundings) are presented. Figure 1(a) corresponds to the case of the absence of dye molecules, while Fig. 1(b) corresponds to their presence. The CLC layer helix is right handed and its pitch is $p = 420\,\text{nm}$. Therefore, the light incident onto a single CLC layer with a right (diffracting) circular polarization (RCP) has a PBG, and the light with left (nondiffracting) circular polarization (LCP) does not. Figure 1(b) corresponds to the case when $\omega_{01} = \omega_{02} = \omega_B = \frac{ac}{\sqrt{\varepsilon_m}}$, that is, when the time resonance frequencies $\omega_{01,2}$ coinciding with spatial Bragg frequency ω_B are considered. Figure 2(b) shows that in the case of the presence of dye molecules the PBG breaks up into two PBGs. It is explained as follows (about the case of more than one PBG, see also [28–31]). The light field in the CLC has the form

$$\vec{E}(z,t) = \sum_{j=1}^{4}[E^+_j\vec{n}_+\exp(ik^+_j z) + E^-_j\vec{n}_-\exp(ik^-_j z)] \times \exp(-i\omega t), \tag{3}$$

where $\vec{n}_\pm = (\vec{x} + i\vec{y})/2$ are the circular polarization orts, and k^+_j and k^-_j are the wave vectors of z components which are connected by the Wolfe-Bragg condition: $k^+_j - k^-_j = 2a$. Here, $k^+_j = 2\pi\sqrt{\varepsilon_m}(\chi \pm b^\pm)/\lambda$, $k^-_j = 2\pi\sqrt{\varepsilon_m}(-\chi \pm b^\pm)/\lambda$, $\chi = \lambda/(p\sqrt{\varepsilon_m})$, λ is the wavelength in vacuum, $b^\pm = \sqrt{1+\chi^2 \pm \gamma}$, and $\gamma = \sqrt{4\chi^2+\delta^2}$. In the PBG the dimensionless wave number b^- must be purely imaginary. Let us

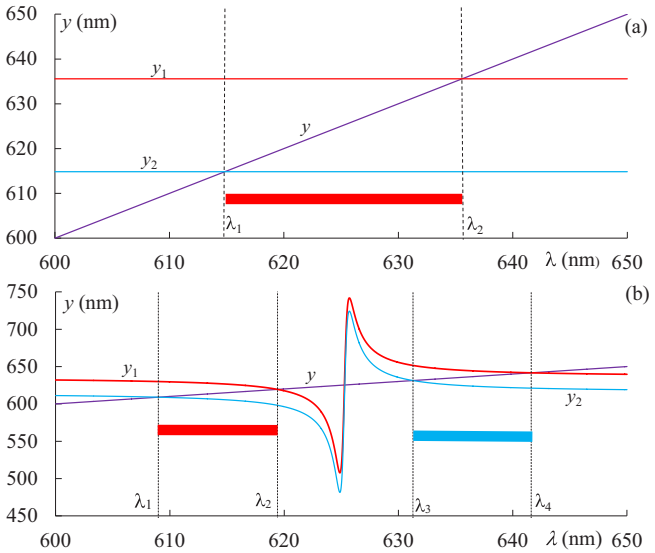

FIG. 2. Dependences $y_1(\lambda)$, $y_2(\lambda)$, and $y(\lambda)$ in the absence (a) and in the presence (b) of dispersion. The parameters are the same as in Fig. 1.

present $b^{\pm}$ in the form

$$b^{\pm} = \sqrt{\left(\frac{b_1 + b_1 + 4\chi^2}{2}\right) \pm \sqrt{\left(\frac{b_1 + b_1 + 4\chi^2}{2}\right)^2 - b_1 b_2}}, \tag{4}$$

where $b_{1,2} = 1 - \chi^2 \pm \delta$. As follows from this presentation, b^- will be purely imaginary if b_1 and b_2 in (4) have different signs. However, this means that PBG borders are the abscissas of intersections of points of the straights $y_1 = p\sqrt{\varepsilon_1}$ and $y_2 = p\sqrt{\varepsilon_2}$ with the straight $y = \lambda$. Between these wavelengths b_1 and b_2 have different signs and $b_1 b_2 = (y_1 - y)(y_2 - y)/(p\sqrt{\varepsilon_m}) < 0$. In accordance with (4), here b^- will be purely imaginary. Therefore, here we have the PBG and its borders coincide with wavelengths $\lambda_1 = p\sqrt{\varepsilon_1}$ and $\lambda_2 = p\sqrt{\varepsilon_2}$. All this is illustrated in Figs. 1(a) and 2(a).

However, if there is a dispersion, then both ε_1 and ε_2 become functions of wavelength λ (or frequency ω), and the straight lines $y_1 = p\sqrt{\varepsilon_1}$ and $y_2 = p\sqrt{\varepsilon_2}$ are replaced by complicated curves $y_1 = p\sqrt{\varepsilon_1(\omega)}$ and $y_2 = p\sqrt{\varepsilon_2(\omega)}$, and consequently, depending on these functions, there can be new regions where the curve $y = \lambda$ lies between curves $y_1 = p\sqrt{\varepsilon_1(\omega)}$ and $y_2 = p\sqrt{\varepsilon_2(\omega)}$. In particular, in the case (2) when $\omega_{01} = \omega_{02} = \omega_B = \frac{ac}{\sqrt{\varepsilon_m}}$ two PBGs arise [Figs. 1(b) and 2(b)]. Of course, there can be situations where there can be more than two PBGs.

For $\lambda_{1,2}$ and $\lambda_{3,4}$ [see Figs. 1(b) and 2(b)], in the condition that ω and ω_0 are of the same order of magnitude and if $|\omega - \omega_0| \gg \gamma$, we will have

$$\lambda_{1,2} = \frac{2\pi c}{\sqrt{\frac{1}{2}\left(\beta_{1,2} + \sqrt{\beta_{1,2}^2 - \frac{\alpha^4}{\varepsilon_m^0 \varepsilon_{1,2}^0}}\right)}},$$

$$\lambda_{3,4} = \frac{2\pi c}{\sqrt{\frac{1}{2}\left(\beta_{1,2} - \sqrt{\beta_{1,2}^2 - \frac{\alpha^4}{\varepsilon_m^0 \varepsilon_{1,2}^0}}\right)}}, \tag{5}$$

where $\alpha = \frac{2\pi c}{p}$, $\beta_{1,2} = \alpha^2 \frac{\varepsilon_{1,2}^0}{\varepsilon_m^0} + \alpha^2 + B$, and $\varepsilon_m^0 = (\frac{\varepsilon_1^0 + \varepsilon_2^0}{2})$.

Now we move onto some new results. We investigate the reflection, transmission, and absorption spectra peculiarities for the two base circular polarizations. Presenting $B = f_1 = f_2$ in the form $B = B_0 + 2\Delta a \times 10^{27}\mathrm{s}^{-2}$ with $B_0 = 1 \times 10^{26}\mathrm{s}^{-2}$, we will investigate the effects of B change on these spectra. In Fig. 3, we present the evolution of the reflection, transmission, and absorption spectra when the parameter B increases. The incident light is RCP (the first row) and LCP (the second row). As can be seen from this figure, with an increase in B, the PBG splits into two regions. With further increase in B, these two regions are removed from each other.

Now presenting $\gamma = \gamma_1 = \gamma_2$ in the form $\gamma = \gamma_0 + 4\Delta\gamma \times 10^{10}\mathrm{s}^{-1}$ with $\gamma_0 = 1 \times 10^{12}\mathrm{s}^{-1}$, we will investigate the effects of γ change on the reflection, transmission, and absorption spectra. In Fig. 4, we present the evolution of these spectra when the parameter γ increases. Again, the incident light is RCP (the first row) and LCP (the second row). As can be seen from this figure, with an increase in γ, light reflection in the two PBGs decreases and their bandwidths decrease too. With further increase in γ, again we have only one PBG where a further decrease in reflection takes place.

Let us now investigate the effect of $\omega_0 = \omega_{01} = \omega_{02}$ on the zone structure of the CLC with dye. Presenting $\lambda_0 = \frac{2\pi c}{\omega_0}$ in the form $\lambda_0 = \lambda_0^0 + \Delta\lambda$ with $\lambda_0^0 = 550\,\mathrm{nm}$, we will investigate the effects of λ_0 change on the reflection, transmission, and absorption spectra. In Fig. 5, we present the evolution of these spectra when the parameter λ_0 increases. Again, the incident light is RCP (the first row) and LCP (the second row). As can be seen from this figure, a change in λ_0 influences both PBG bandwidth and the amount of PBSs.

Finally, let us now investigate the effect of CLC layer thickness d on the reflection R, transmission T, and absorption A spectra. In Fig. 6, we present the evolution of these spectra when d increases. Again, the incident light is RCP (the first row) and LCP (the second row).

Now we investigate the peculiarities of light localization in the CLC layer with dye molecules. Let us note that the ability to trap light by optical systems is important both from a scientific point of view as well as from a technological one. Many light trapping methods exist, but they all achieve light trapping with materials or systems that forbid outgoing waves. These systems can be implemented by metallic mirrors, by photonic band-gap materials [32], by highly disordered media (Anderson localization) [33], by nonreciprocally reflected or asymmetrically transmitted systems [34], etc. The total electric field in each medium (we discuss a CLC layer sandwiched between two isotropic half spaces) can be presented as follows:

$$\vec{E}^0(z) = \vec{E}_i(z) + \vec{E}_r(z),\ \vec{E}^1(z) = \vec{E}^{\mathrm{in}}(z),\ \vec{E}^2(z) = \vec{E}_t(z), \tag{6}$$

where the indices zero, one, and two denote the fields corresponding to the medium on the left-hand side of the CLC layer, the CLC layer, and the medium on the right-hand side of the CLC layer, respectively. $\vec{E}_i$, $\vec{E}_r$, and $\vec{E}_t$ are the fields of the incident, reflected, and transmitted waves, respectively, and $\vec{E}^{\mathrm{in}}$ is the total field in the CLC layer, with the z axis directed along the axis of the CLC helix. In Fig. 7, we display the change in the spectra of total field intensity $|\vec{E}^{0,1,2}(z)|^2$, and total field ellipticity e, when the coordinate z changes, in the

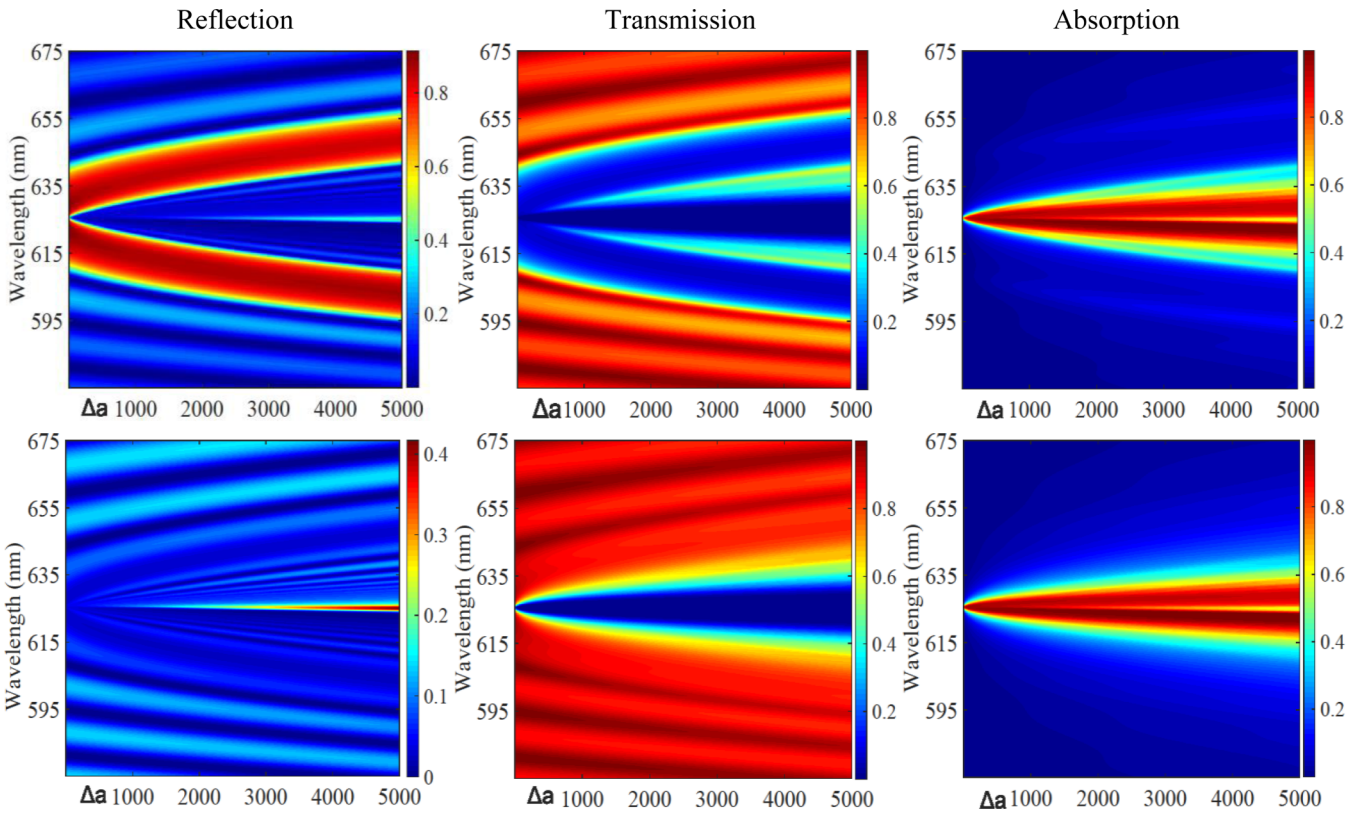

FIG. 3. The evolution of the reflection, transmission, and absorption spectra when the parameter B increases. The incident light is RCP (the first row) and LCP (the second row). $d = 20p$. The other parameters are the same as in Fig. 1.

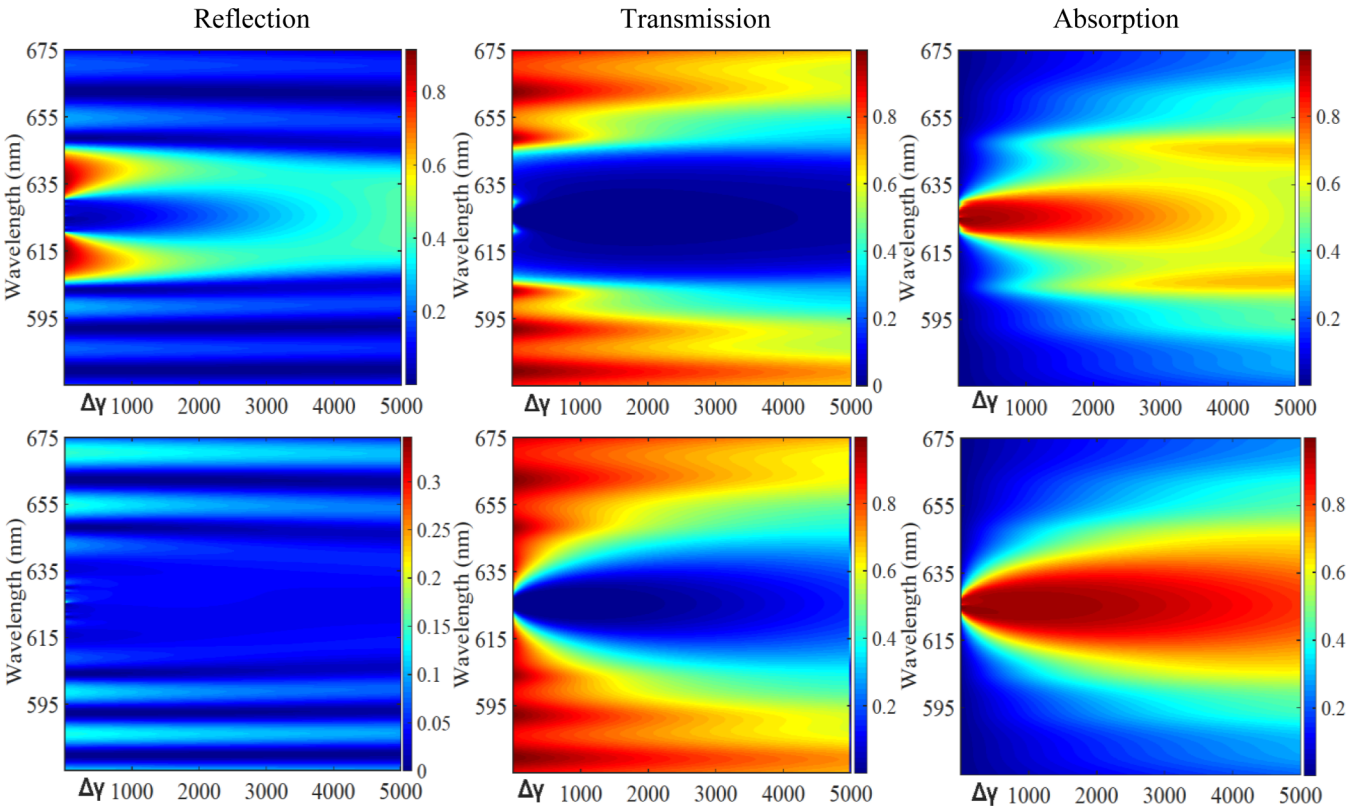

FIG. 4. The evolution of the reflection, transmission, and absorption spectra when the parameter γ increases. The incident light is RCP (the first row) and LCP (the second row). $d = 20p$. The other parameters are the same as in Fig. 1.

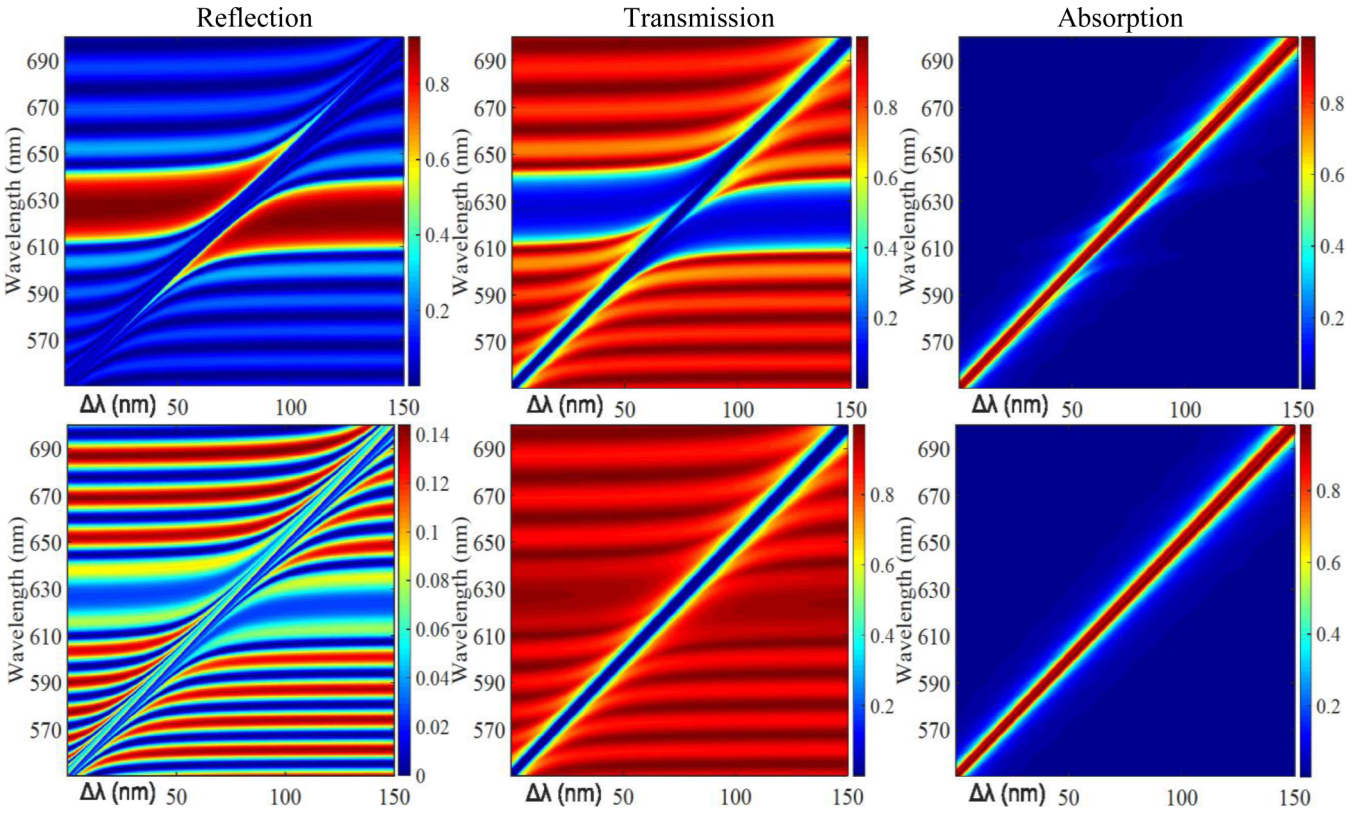

FIG. 5. The evolution of the reflection, transmission, and absorption spectra when the parameter λ_0 increases. The incident light is RCP (the first row) and LCP (the second row). $d = 20p$. The other parameters are the same as in Fig. 1.

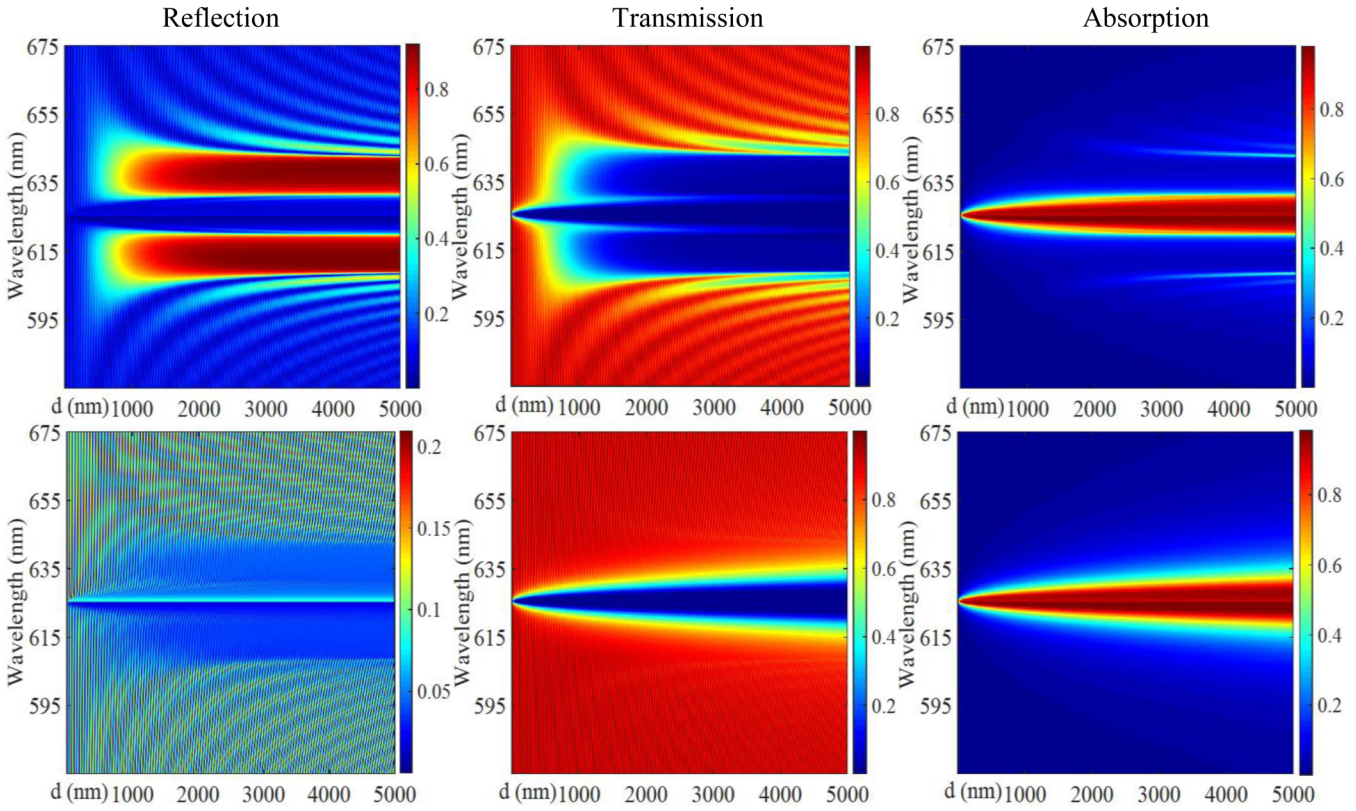

FIG. 6. The evolution of the reflection R, transmission T, and absorption A spectra when the CLC layer thickness d increases. The incident light is RCP (the first row) and LCP (the second row). The other parameters are the same as in Fig. 1.

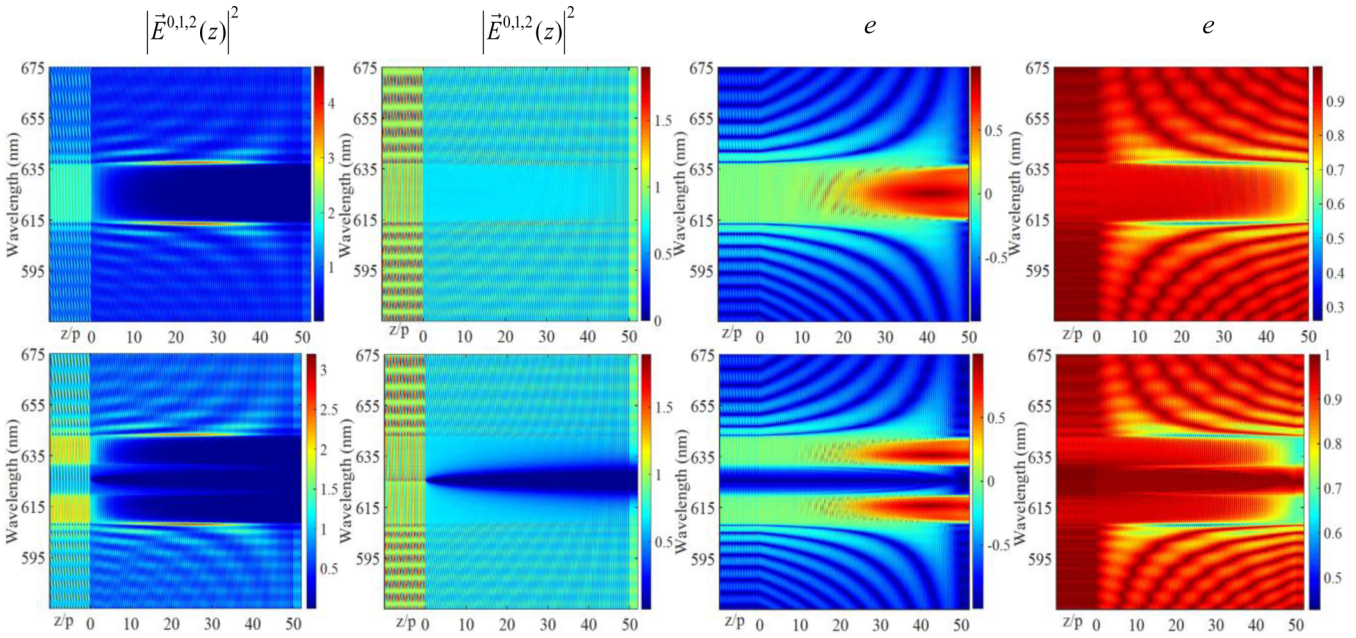

FIG. 7. The change in the spectra of total field intensity $|\vec{E}^{0,1,2}(z)|^2$ (the first and the second columns), and total field ellipticity e (the third and the fourth columns), when the coordinate z changes, in the case of absence of dye molecules in the CLC (the first row). The second row presents the same dependences in the case of the presence of dye molecules in the CLC. The incident light has the polarization coinciding with RCP (the first and the third columns) and LCP (the second and the fourth columns). The parameters are the same as in Fig. 1.

case of absence of dye molecules in the CLC (the first row). The second row presents the same dependences in the case of the presence of dye molecules in the CLC. The incident light has the polarization coinciding with RCP (the first and third columns) and LCP (the second and the fourth columns). The CLC layer occupies the space (area) between the planes $z = 0$ and $50p$. As it is seen from these figures, strong localization of light takes place for the light corresponding to the right (diffracting) CP and at frequencies near the boundaries of the PBG (occupying the area from 615 to 635 nm). These frequencies coincide with the frequencies of the minima of the reflection coefficient, and for $\varepsilon_s = \varepsilon_m$ they are approximately determined from the condition

$$kd = 2\pi m, \quad m = \pm 1, \pm 2, \pm 3 \ldots, \tag{7}$$

where $k = \frac{2\pi}{\lambda}\sqrt{\varepsilon_m(1 + \chi^2 - \sqrt{4\chi^2 + \delta^2})}$ and $\chi = \frac{\lambda}{p\sqrt{\varepsilon_m}}$.

For $\varepsilon_s \neq \varepsilon_m$, the condition (7) has a more complicated form. At these frequencies (called edge-mode frequencies), the effects of anomalously strong absorption and emission occur, as well as low-threshold laser generation (see, in particular, [35–38], and references cited therein). As far as the order of the edge modes increases, the localization decreases. Some localization on these modes is also observed when light falls on a layer with a left (nondiffracting) CP.

Then, as it is well known, in the case of minimal influence of CLC layer dielectric borders (that is, when $\varepsilon_s = \varepsilon_m$) and in the case of normal light incidence and if it has the diffracting circular polarization, the total standing wave field excited in the medium is linearly polarized in the PBG. Moreover, the total field direction is fixed, for a fixed coordinate along the axis of the helix. As the coordinate z (directed along the medium axis) changes, this direction rotates around z in such a way that the angle between the director at each point and this direction remains the same. If the light frequency changes, the angle between the director and total field also changes. As follows from these dependences in the case $\varepsilon_s = 1$ some differences appear; for example, at large values of z the total field already does not have linear polarization.

The averaged light energy density in the CLC layer can be calculated by the following formula:

$$w = \frac{1}{d}\int_0^d |\vec{E}^1(z)|^2 dz,$$

and the photonic density of states (PDS) can be calculated by the following:

$$\rho_i(\omega) \equiv \frac{dk_i}{d\omega} = \frac{1}{d}\frac{\frac{du_i}{d\omega}v_i - \frac{dv_i}{d\omega}u_i}{{u_i}^2 + {v_i}^2}, \quad i = 1, 2,$$

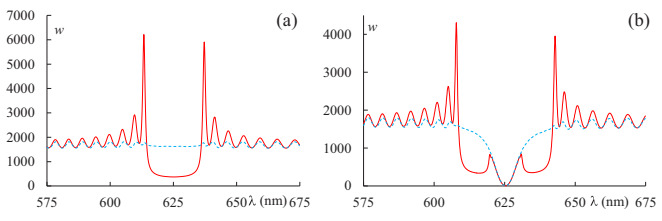

FIG. 8. The light energy density w spectra in the case of absence of dye molecules (a) and in the case of their presence (b). The incident light is RCP (the red solid lines) and LCP (the blue dashed lines). The parameters are the same as in Fig. 1.

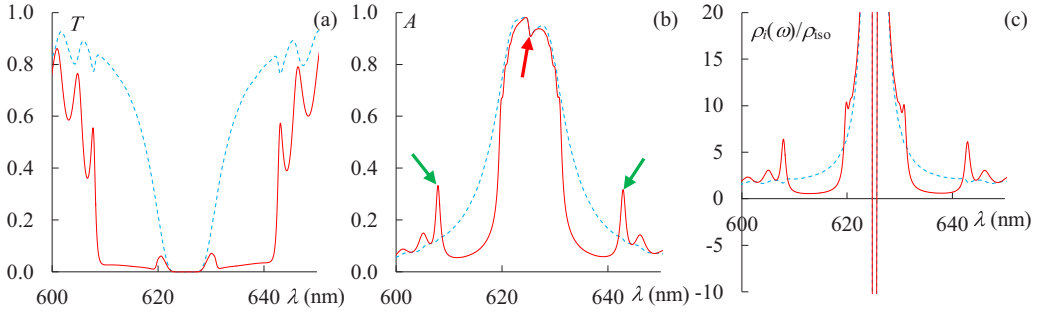

FIG. 9. The transmission T (a), the absorption $A = 1 - (R + T)$(b), and the normalized PDS $\rho_i(\omega)/\rho_{iso}$ with $\rho_{iso} = \frac{\sqrt{\varepsilon_s}}{c}$ (c) spectra in the presence of dye molecules. The incident light is RCP (the red solid lines) and LCP (the blue dashed lines). The parameters are the same as in Fig. 1.

where d is the CLC layer thickness, and u_i and v_i are the real and imaginary parts of $T_i(\omega) = u_i(\omega) + iv_i(\omega)$ transmission coefficients for the incident light with both strongly and weakly diffracting eigenpolarizations (EPs). The EPs are the two polarizations of the incident light, which do not change when light transmits through the system. As it is known (in particular, at the normal incidence) the EPs of either CLC or gyrotropic media practically coincide with the orthogonal circular polarizations; meanwhile, they coincide with the orthogonal linear polarizations for the nongyrotropic media [39].

Figure 8 presents the light energy density w spectra in the case of absence of dye molecules [Fig. 8(a)], and in the case of their presence [Fig. 8(b)]. As can be seen from Fig. 8(a), w has maxima on edge modes and it is minimum in the PBG. In the presence of dye molecules $w \to 0$ on the wavelength of resonance λ_0.

Figure 9 presents the transmission T (a), the absorption $A = 1 - (R + T)$(b), and the normalized PDS $\rho_i(\omega)/\rho_{iso}$ with $\rho_{iso} = \frac{n_s}{c}$ (c) spectra. As can be seen from Fig. 9(b), in two PBGs, depending on the polarization of the incident light, the absorption suppression effect of Bormann and anomalously strong absorption effect were observed (in this figure, two absorption maxima of this type are indicated by green arrows). These effects are due to the diffraction of light on the periodical structure of a medium (which manifests itself in an appearance of the polarization dependent PBG) and diffraction of light in limited volume (which manifests itself in the appearance of oscillations outside the PBG). Near the wavelength λ_0 superstrong absorption takes place due to time dispersion. Let us note the dip in the absorption spectrum at the very wavelength λ_0 in the absorption spectrum (in this figure, this dip is indicated by a red arrow).

To conclude this section, let us note that in the CLC it is possible to obtain the PBG in the desired frequency region by introducing dye molecules into the CLC matrix. This requirement imposes a condition on the strength of the oscillator and on the frequency of the absorption line of dye molecules. Naturally, all these opportunities enlarge the possible limits and regions of application of the CLC with dye molecules.

IV. FANO RESONANCE IN THE CLC WITH DYE

As can be seen from Fig. 1(b), near the resonant wavelength λ_0, a reflection independent of the polarization is observed, and the reflection profile has a form similar to the

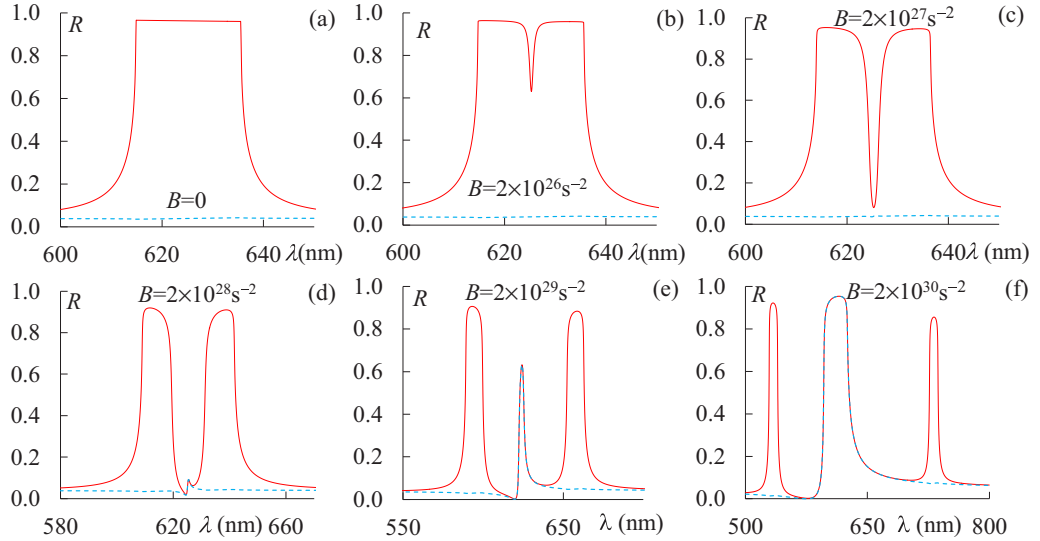

FIG. 10. The reflection R spectra at different values of B. $\gamma = 4 \times 10^{12}\ s^{-1}$. The incident light is RCP (the red solid lines) and LCP (the blue dashed lines). The other parameters are the same as in Fig. 1.

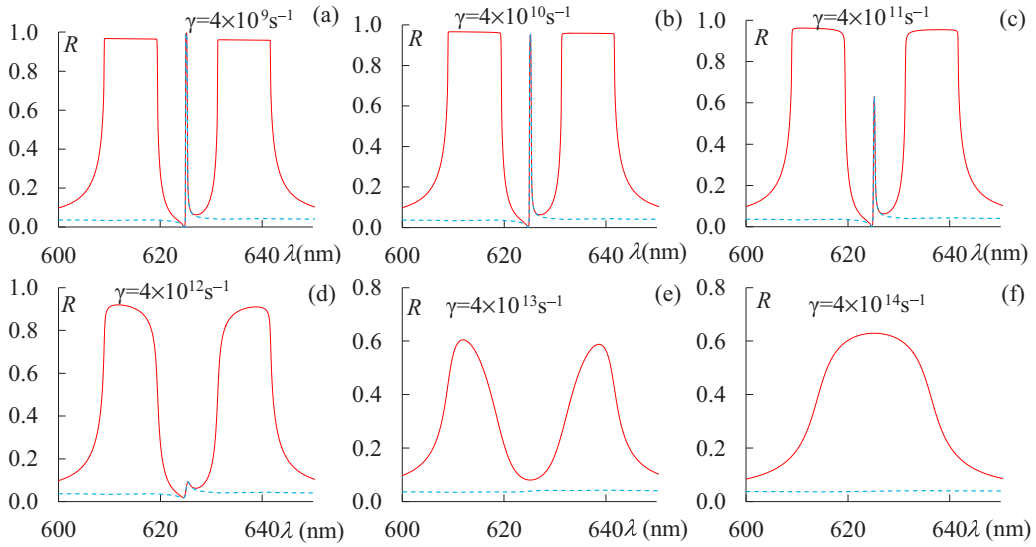

FIG. 11. The reflection R spectra at different values of γ. $B = 2 \times 10^{28}\ \mathrm{s}^{-2}$. The incident light is RCP (the red solid lines) and LCP (the blue dashed lines). The other parameters are the same as in Fig. 1.

symmetric form of the Lorentz resonance. Here we have the interaction of two resonances, the Bragg type resonance on the periodical structure of CLC and resonance due to time dispersion, and therefore here we must observe the Fano resonance effect. As it is known, the asymmetric Fano contour arises as a result of the interaction of a narrow resonance with a wide contour. Now consider the reflection of light from the planar half space of the CLC. Figure 10 presents the reflection R spectra at different values of B. As can be seen from Fig. 10, with increasing of B, a dip appears in the reflection spectrum. Then the depth of this dip increases. Starting with a certain value of B, the reflection spectrum around λ_0 has a form similar to the symmetric form of the Lorentz resonance. With a further increase of B, the reflection spectrum around λ_0 acquires a characteristic Fano resonance asymmetric shape.

Figure 11 presents the reflection R spectra at different values of γ. At small values of γ, the reflection spectrum has a characteristic Fano resonance asymmetric shape. When γ increases, it acquires a characteristic Lorentz resonance symmetric shape. With further increase of γ, the resonance nature of the reflection spectrum around λ_0 decreases.

In order to investigate the transmission and absorption features in the above-considered intervals for the variation of the quantities B and γ, we again return to the problem for the finite CLC layer. In Fig. 12 we present reflection R, transmission T, and absorption A spectra corresponding to the cases in Fig. 10(e) [Figs. 12(a)–12(c)] and Fig. 11(b) [Figs. 12(d)–12(f)]. As can be seen from Fig. 12, in the case of a finite CLC layer the reflection spectrum around λ_0 has a form similar to the asymmetric shape of the Fano

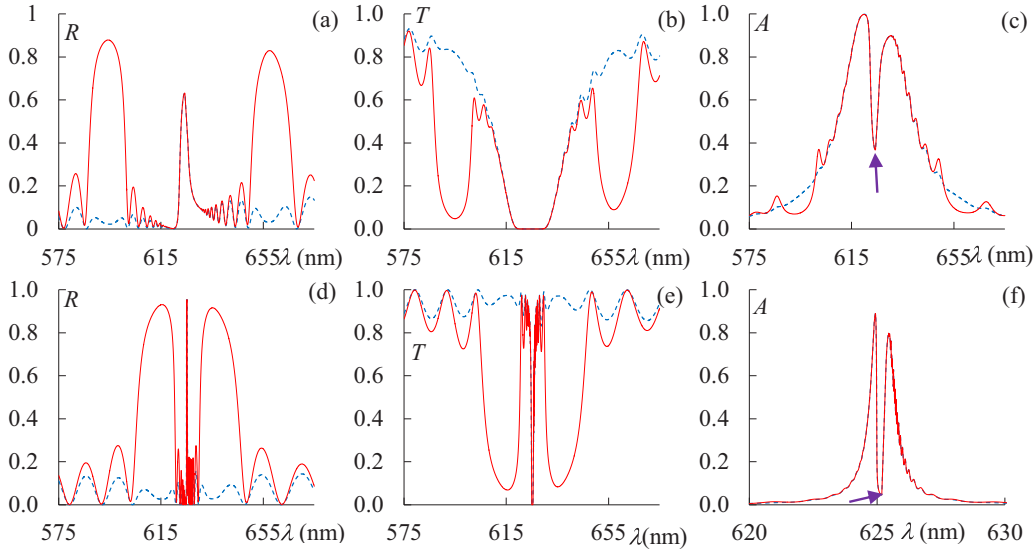

FIG. 12. The reflection R, transmission T, and absorption A spectra. (a–c) $B = 2 \times 10^{29}\ \mathrm{s}^{-2}$ and $\gamma = 4 \times 10^{10}\ \mathrm{s}^{-1}$. (d–f) $B = 2 \times 10^{28}\ \mathrm{s}^{-2}$ and $\gamma = 4 \times 10^{12}\ \mathrm{s}^{-1}$. $d = 20p$. The incident light is RCP (the red solid lines) and LCP (the blue dashed lines). The other parameters are the same as in Fig. 1.

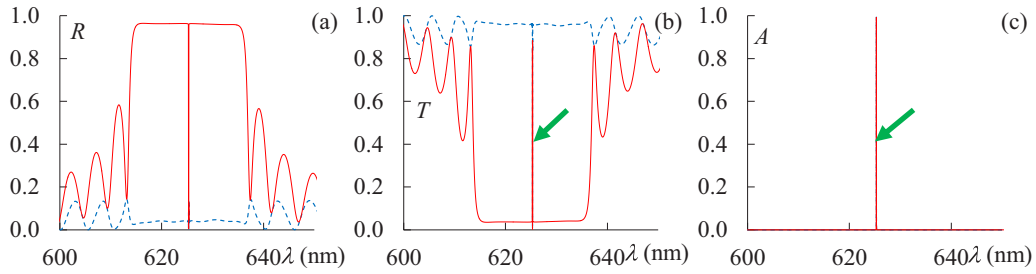

FIG. 13. The reflection R, transmission T, and absorption A spectra at $B = 1 \times 10^{26}\ \mathrm{s}^{-2}$ and $\gamma = 4 \times 10^{8}\ \mathrm{s}^{-1}$. $d = 50p$. The incident light is RCP (the red solid lines) and LCP (the blue dashed lines). The other parameters are the same as in Fig. 1.

resonance. Dips in the spectra of absorption in both cases are due to strong reflection [in Figs. 12(c) and 12(f) these dips are indicated by purple arrows]. However, here high reflection is due not to periodical photonic structure but to high values of the attenuation coefficient and high refraction index (that is, this reflection is similar to reflection from a metallic surface). As can be seen from Fig. 12, the absorption curves also are asymmetric around λ_0. This is due to the following circumstances:

(1) With wide absorption lines, $T \approx 0$ around λ_0 and here the absorption repeats the asymmetric form of reflection R.

(2) A certain contribution in this asymmetric form of absorption A also has the dependence of the attenuation $\mathrm{Im}k = \frac{2\pi}{\lambda}\mathrm{Im}n$ on the wavelength λ.

Then, with ultranarrow absorption lines, a supernarrow PBG can be formed around λ_0 (see also below). Let us note that a certain asymmetry also exists in the dependences of $|\vec{E}^1(z)|^2$ and w on the wavelength λ. This asymmetry in the scale of the graphs in Figs. 7 and 8 is not expressed.

As was shown above, under certain conditions, a gap appears in the absorption line around λ_0. Such a gap appears also when electromagnetically induced transparency takes place. However, if in our case this is due to the narrow-band mirrorlike reflection, then in the second case a narrow-band transmission line appears. Moreover, as we show in our investigations, for certain values of B and γ, we can observe the effect of the appearance of narrow-band lines of total transmission in the immediate vicinity of a narrow-band full absorption line. Figure 13 presents reflection R, transmission T, and absorption A spectra corresponding to the case $B = 1 \times 10^{26}\ \mathrm{s}^{-2}$ and $\gamma = 4 \times 10^{8}\ \mathrm{s}^{-1}$. The peaks in the transmission and absorption spectra (indicated by green arrows) take place in neighboring wavelengths. As we show in our investigations, in this case a supernarrow PBG arises around λ_0. Let us note that these narrow transmission lines can be used as narrow bandpass filters.

V. CONCLUSIONS

In conclusion, we investigated the optical properties of CLCs in the presence of dispersion in local components of the dielectric tensor. Such a situation can take place, for instance, in the presence of dye molecules in the CLC matrix. It was shown that in the presence of dye molecules, in certain conditions, the PBG splits into two, three, etc., PBGs. We offered simple geometrical and analytical methods to determine Bragg frequencies and frequency boundaries of these forbidden bands. Then we investigated the effects of dispersion parameters and CLC layer thickness on the band structure peculiarities. We showed that in the CLC it is possible to obtain the PBG in the desired frequency region by introducing dye molecules into the CLC matrix. This requirement imposes a condition on the strength of the oscillator and on the frequency of the absorption line of dye molecules. We showed that in the presence of the two types of resonances, resonance due to spatial periodical structure (Bragg resonance) and resonance due to time dispersion (Lorentz resonance), the observation of Fano resonance is possible, due to the interference of these two resonances. The peculiarities of Fano resonance in CLCs with dyes were investigated.

[1] U. Fano, Phys. Rev. **124**, 1866 (1961).
[2] Luk'yanchuk, N. I. Zheludev, S. A. Maier, N. J. Halas, P. Nordlander, H. Giessen, and C. T. Chong, Nat. Mater. **9**, 707 (2010).
[3] A. E. Miroshnichenko, S. Flach, and Y. S. Kivshar, Rev. Mod. Phys. **82**, 2257 (2010).
[4] A. Hessel and A. A. Oliner, Appl. Opt. **4**, 1275 (1965).
[5] M. Sarrazin, J. P. Vigneron, and J. M. Vigoureux, Phys. Rev. B **67**, 085415 (2003).
[6] M. F. Limonov, M. V. Rybin, A. N. Poddubny, and Y. S. Kivshar, Nat. Photon. **11**, 543 (2017).
[7] J. A. Chen *et al.*, Science **328**, 1135 (2010).
[8] V. Giannini *et al.*, Nano Lett. **11**, 2835 (2011).
[9] S. Zhang, K. Bao, N. J. Halas, H. Xu, and P. Nordlander, Nano Lett. **11**, 1657 (2011).
[10] M. Rahmani *et al.*, Nanotechnology **22**, 245204 (2011).
[11] C. P. Holfeld, F. Loser, M. Sudzius, K. Leo, D. M. Whittaker, and K. Kohler, Phys. Rev. Lett. **81**, 874 (1998).
[12] S. Fan, Appl. Phys. Lett. **80**, 908 (2002).
[13] E. Miroshnichenko and Y. S. Kivshar, Opt. Express **13**, 3969 (2005).
[14] M. V. Rybin, A. B. Khanikaev, M. Inoue, K. B. Samusev, M. J. Steel, G. Yushin, and M. F. Limonov, Phys. Rev. Lett. **103**, 023901 (2009).
[15] S. Fan, W. Suh, and J. D. Joannopoulos, J. Opt. Soc. Am. A **20**, 569 (2003).

[16] H. Yang *et al.*, Appl. Phys. Lett. **95**, 023110 (2009).
[17] F. Patthey, M. H. Schaffner, W. D. Schneider, and B. Delley, Phys. Rev. Lett. **82**, 2971 (1999).
[18] Y.-F. Xiao, M. Li, Y.-C. Liu, Y. Li, X. Sun, and Q. Gong, Phys. Rev. A **82**, 065804 (2010).
[19] A. R. Cowan and J. F. Young, Phys. Rev. E **68**, 046606 (2003).
[20] F. Mingaleev, A. E. Miroshnichenko, and Y. S. Kivshar, Opt. Express **16**, 11647 (2008).
[21] A. E. Miroshnichenko, Y. Kivshar, C. Etrich, T. Pertsch, R. Iliew, and F. Lederer, Phys. Rev. A **79**, 013809 (2009).
[22] S.-C. Jeng, S.-J. Hwang, Y.-H. Hung, and S.-C. Chen, Opt. Express. **18**, 22572 (2010).
[23] A. H. Gevorgyan, M. Z. Harutyunyan, A. Kocharian, and G. A. Vardanyan, Mol. Cryst. Liq. Cryst. **432**, 69 (2005).
[24] E. L. Ivchenko and A. N. Poddubny, Phys. Solid State **55**, 905 (2013).
[25] S. Ya. Vetrov, A. Yu. Avdeeva, and I. V. Timofeev, J. Exp. Theor. Phys. **113**, 755 (2011).
[26] A. A. Gevorgyan, Opt. Spectrosc. **89**, 631 (2000).
[27] A. H. Gevorgyan, Mod. Phys. Lett. B **24**, 921 (2010).
[28] A. H. Gevorgyan, Ph.D. thesis, Yerevan State University, 1987.
[29] A. H. Gevorgyan, Izv. Acad. Sci. Arm. SSR, Fizika **18**, 132 (1983).
[30] J. Wang, A. Lakhtakia, and J. B. Geddes III, Optik **113**, 213 (2002).
[31] A. Lakhtakia and J. T. Moyer, Optik **113**, 97 (2002).
[32] J. D. Joannopoulos, S. G. Johnson, J. N. Winn, and R. D. Meade, *Photonic Crystals: Molding the Flow of Light*, 2nd ed. (Princeton University Press, Princeton, NJ, 2008).
[33] A. Lagendijk, B. van Tiggelen, and D. Wiersma, Phys. Today **62**, 24 (2009).
[34] A. H. Gevorgyan, A. Kocharian, and G. A. Vardanyan, Opt. Commun. **259**, 455 (2006).
[35] V. A. Belyakov, A. A. Gevorgian, O. S. Eritsian, and N. V. Shipov, Zhurn. Tekhn. Fiz. **57**, 1418 (1987) [Sov. Phys. Tech. Phys. **32**, 843 (1987)].
[36] V. A. Belyakov and S. V. Semenov, J. Exp. Theor. Phys. **109**, 687 (2009).
[37] A. H. Gevorgyan, J. Contemp. Phys. **50**, 28 (2015).
[38] V. I. Kopp, Z.-Q. Zhang, and A. Z. Genack, Prog. Quantum Electron. **27**, 369 (2003).
[39] A. H. Gevorgyan, Phys. Rev. E **83**, 011702 (2011).